Introduction

Regenerative braking is a key technology in electric vehicle design, as it allows energy to be recovered during braking, improving efficiency and extending battery life. This report focuses on the design and analysis of a regenerative braking system (Emadi A., 2015).

The study is divided into three main parts. First, a DC-AC inverter circuit is examined to understand energy conversion (Ojo O., 2004). Second, the regenerative braking circuit is analysed and redesigned to include ultracapacitors, DC-DC converters (Hedlund M. 2010) and improved power management. Finally, the practical limitations of these systems are assessed, and improvements are proposed.

Part A: DC-AC Inverter

Circuit diagram

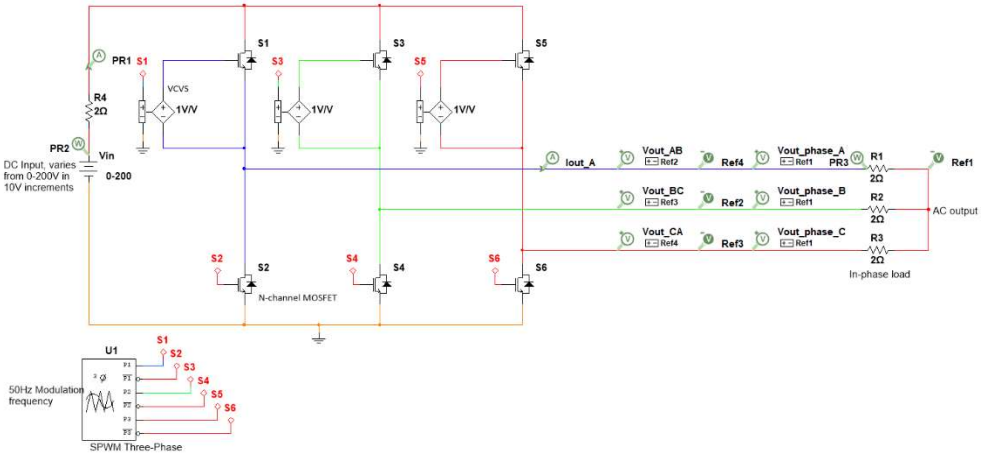

Figure 1. DC-AC Inverter circuit diagram

The operation of a DC-AC three-phase inverter consists of a DC voltage source, which provides the circuit with a voltage which, through the use of a set of transistors, is transformed into a three-phase AC signal.

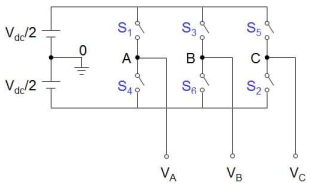

Figure 2. PWM circuitry

To allow the use of the transistors, a Sinusoidal Pulse-Width Modulation (SPWM) technique is used, changing the state of the transistors and thus, the output phase voltage (García J., 2023).

These transistors can be either MOSFETs or IGBTs (Ojo O., 2004). For these, when a voltage above the imposed threshold is applied to the gate, the transistor turns ON, creating a path between the drain and the source, otherwise, the transistor remains OFF.

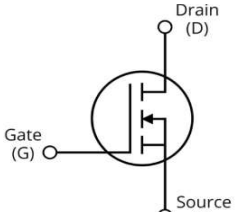

Figure 3. N-channel Enhancement MOSFET

These are used in an H-bridge configuration in a DC-AC inverter, utilising pairs of transistors for each phase, switching their state, in order to create the AC wave.

The correct switching of the transistors is vital to the operation of the circuit, as if both transistors present in the same phase are ON at the same time, a short circuit will occur.

The theoretical options of activation of the transistors are the following (Ojo O., 2004):

Table 1. Positive-signal transistors Switching sequence

S1	S3	S5	V_{AB}	V_{BC}	V_{CA}
0	0	0	0	0	$-V_{DC}/2$
0	0	1	$-V_{DC}/\sqrt{3}$	$V_{DC}/\sqrt{3}$	$-V_{DC}/6$
0	1	0	$-V_{DC}/3$	$-V_{DC}/\sqrt{3}$	$-V_{DC}/6$
0	1	1	$-2V_{DC}/3$	0	$V_{DC}/6$
1	0	0	$2V_{DC}/3$	0	$-V_{DC}/6$
1	0	1	$V_{DC}/3$	$-V_{DC}/\sqrt{3}$	$V_{DC}/6$
1	1	0	$V_{DC}/3$	$V_{DC}/\sqrt{3}$	$V_{DC}/6$
1	1	1	0	0	$V_{DC}/2$

To measure the input power, a resistor is placed in front of the DC source in order to obtain the maximum power output. To determine the input and load resistances, the maximum load transfer theorem is used (Fraile J., 2012).

$$P_L = R_L \frac{U_{th}^2}{(R_{th} + R_L)^2} \; ; \; \frac{dP_L}{dR_L} = 0 \; ; \; R_L = R_{Th}$$

To determine the value of the resistors, we consider the maximum current allowed by the cables and the high-power demands of the circuits. To meet our requirements, an impedance of 2Ω is selected for both input and load resistors.

For improved control of the positive-signal transistors, providing a direct path to ground, Voltage-Controlled Voltage Sources (VCVS) are implemented. These improve circuit behaviour by enhancing the PWM input to the gate, while, in this particular circuit, providing a direct path to ground for the transistors.

Simulation results

To obtain the switching pattern of the SPWN, we can compare the reference signals, V_A, V_B and V_C with the triangular signal, V_T. When the reference signals intersect with V_T, the inverter switches state (Ojo O., 2004). These intersecting moments and SPWM switching pattern are presented as two oscilloscope measurements.

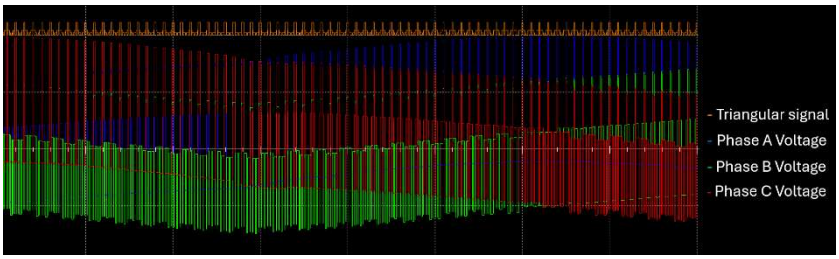

Figure 4. Oscilloscope view of V_T, V_A, V_B and V_C

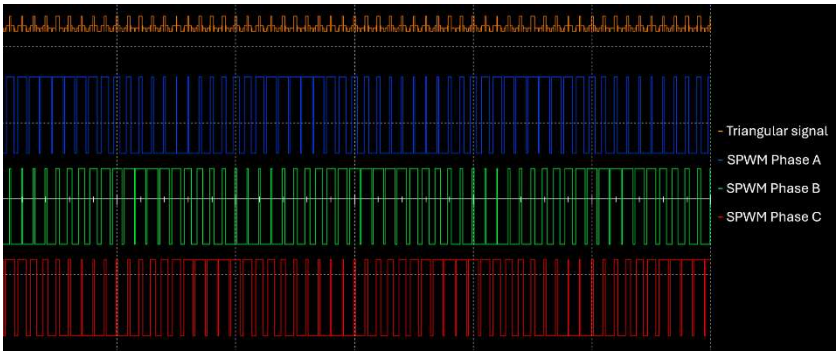

Figure 5. Oscilloscope offset view of the SPWM and triangular signals

After varying the input voltage between 0-200V in 10V intervals, we obtain the following measurements (Bird, J., 2021):

$$P_{in,D.C.} = V_{in} * I_{in}$$

$$P_{out,A.C.} = \sqrt{3} * rms(V_{phase}\quad) * rms(I_{phase}\ )$$

Table 2. Measured values taken from the DC/AC inverter

Input Voltage	Input Current	Input Power	Output Current	Output Line Voltage	Output Phase Voltage	Output Power	Eficiency
10 V	1.63 A	16.33 W	1.15 A	2.30 V	4.00 V	7.96 W	48.75%
20 V	3.27 A	65.31 W	2.30 A	4.60 V	7.99 V	31.84 W	48.75%
30 V	4.90 A	146.94 W	3.45 A	6.90 V	11.99 V	71.64 W	48.75%
40 V	6.53 A	261.23 W	4.60 A	9.20 V	15.98 V	127.35 W	48.75%
50 V	8.16 A	408.17 W	5.75 A	11.50 V	19.98 V	198.99 W	48.75%
60 V	9.80 A	587.77 W	6.90 A	13.80 V	23.97 V	286.54 W	48.75%
70 V	11.43 A	800.01 W	8.05 A	16.10 V	27.97 V	390.02 W	48.75%
80 V	13.06 A	1044.90 W	9.20 A	18.40 V	31.97 V	509.41 W	48.75%
90 V	14.69 A	1322.50 W	10.35 A	20.70 V	35.96 V	644.72 W	48.75%
100 V	16.62 A	1632.70 W	11.50 A	23.00 V	39.96 V	795.95 W	48.75%
110 V	17.96 A	1975.50 W	12.65 A	25.30 V	43.95 V	963.11 W	48.75%
120 V	19.59 A	2351.10 W	13.80 A	27.60 V	47.95 V	1146.20 W	48.75%
130 V	21.22 A	2759.20 W	14.95 A	29.90 V	51.95 V	1345.20 W	48.75%
140 V	22.86 A	3200.10 W	16.10 A	32.20 V	55.94 V	1560.10 W	48.75%
150 V	24.49 A	3673.50 W	17.25 A	34.50 V	59.94 V	1790.90 W	48.75%
160 V	26.12 A	4179.70 W	18.40 A	36.80 V	63.93 V	2037.60 W	48.75%
170 V	27.59 A	4663.10 W	19.44 A	38.87 V	67.53 V	2273.30 W	48.75%
180 V	29.39 A	5289.90 W	20.70 A	41.40 V	71.92 V	2578.90 W	48.75%
190 V	31.02 A	5894.00 W	21.85 A	43.70 V	75.92 V	2873.40 W	48.75%
200 V	32.65 A	6530.70 W	23.00 A	46.00 V	79.92 V	3183.80 W	48.75%

Following the maximum power transfer theorem, the maximum possible efficiency should be 50% (Abdallah, 2016). As the efficiency of the circuit is close to 50%, we can confirm the proper application of the theorem.

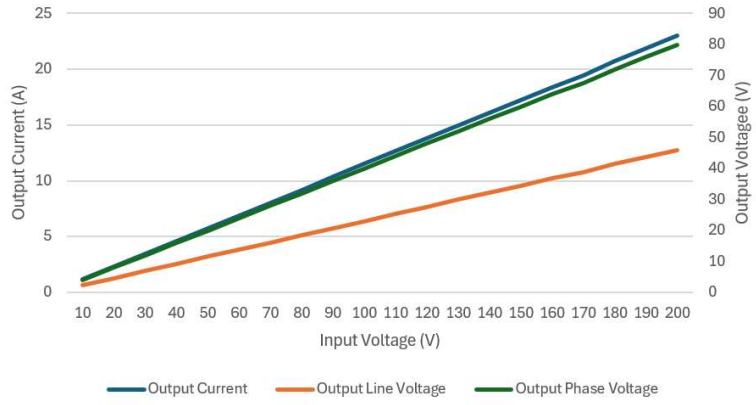

Figure 6. Output voltages and current

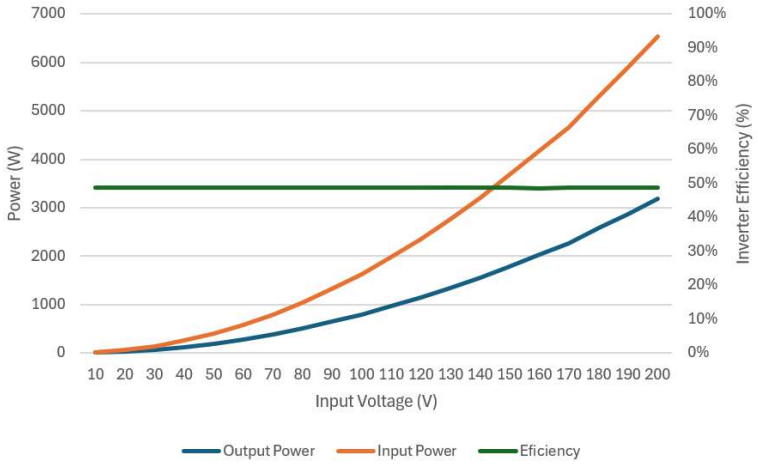

Figure 7. Power and efficiency results

We can observe a linear increase in output voltage and current as the input voltage increases, which in turn creates a parabolic evolution in both input and output power.

As this circuit operates under ideal conditions, heat transfer losses and conductivity resistance are not considered, which translates into the same inverter efficiency regardless of the input voltage, as seen in the recorded results and discussed in this report.

Part B: Regenerative Braking System

Circuit diagram

Following the block diagram for a low-speed regenerative braking system (Nama T., 2022), a circuit is created.

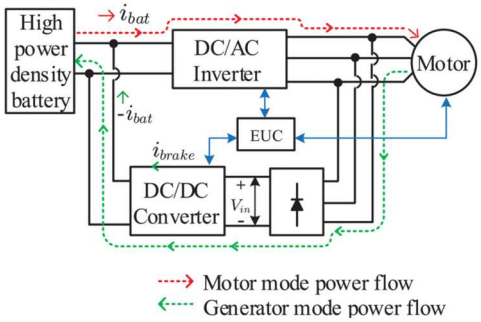

Figure 8. Block diagram of low-speed regenerative braking topology

Although an operational design should include capacitances of 50F (Mishra S., 2023), to ease the simulation, a battery pack of 0.1F and an ultra-capacitor of 0.05F have been used, as well as a series of switches, replacing the proposed controller, allowing manual selection of the charge, discharge and hold phases, and the use of the battery, ultra-capacitor, or both.

Since the regenerative braking system and the energy output of the battery follow separate paths, we can ensure that the battery can continue to supply power to the motor in the event of a failure of the regenerative system.

A Buck converter boosts the current output, while a Boost converter boosts the voltage (Hedlund M., 2010). For this reason, a Boost converter is used on the regenerative braking phase, while a Buck converter on the powering phase, in order to increase the capacitor charge and the output torque, respectively.

A speed of 69 rad/s was selected for the load, in order to simulate a vehicle with 16” wheels driving at 50km/h.

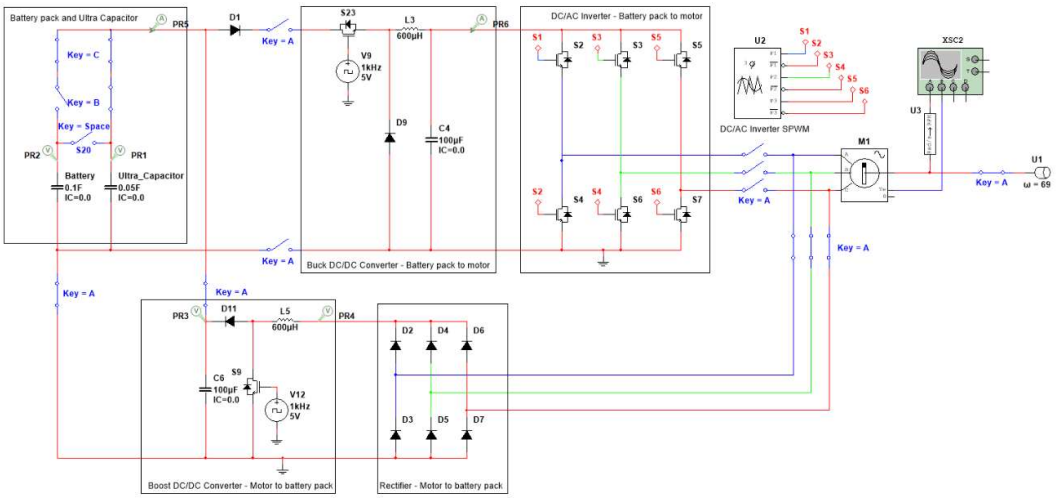

Figure 9. Proposed regenerative braking circuit diagram

Simulation results

Using oscilloscopes, we can observe the change of state of charge of both the battery pack and the ultracapacitor, as well as the effect that the different states have on the motor´s electromagnetic torque and rpm.

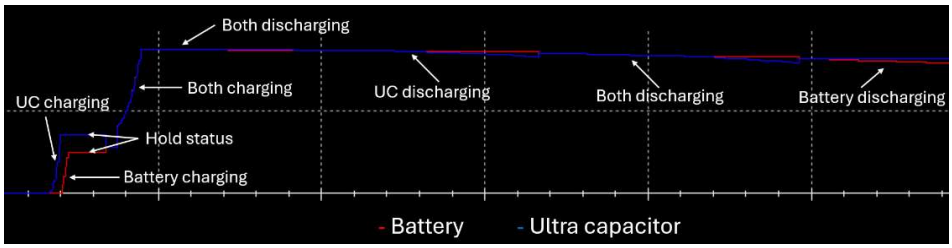

Figure 10. Battery pack charge and discharge state

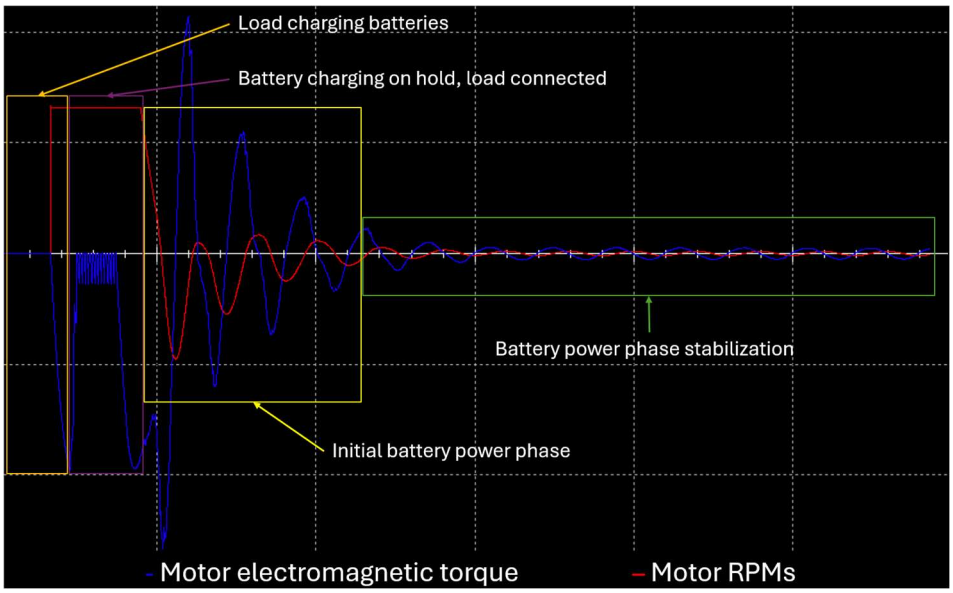

Figure 11. Synchronous motor electromagnetic torque and RPMs

In the initial stages of the battery powering phase, the torque´s amplitude is significantly greater than on the later stabilized phase. This emphasises the need for an ultracapacitor, as it can aid the battery on covering this additional power needed for the initial stage, reducing battery strain and improving the system´s response.

Additionally, we can observe that, for the Boost DC-DC converter, the output voltage is higher than the input voltage, while for the Buck DC-DC converter, the output current is higher than the input current, confirming the correct operation of both converters.

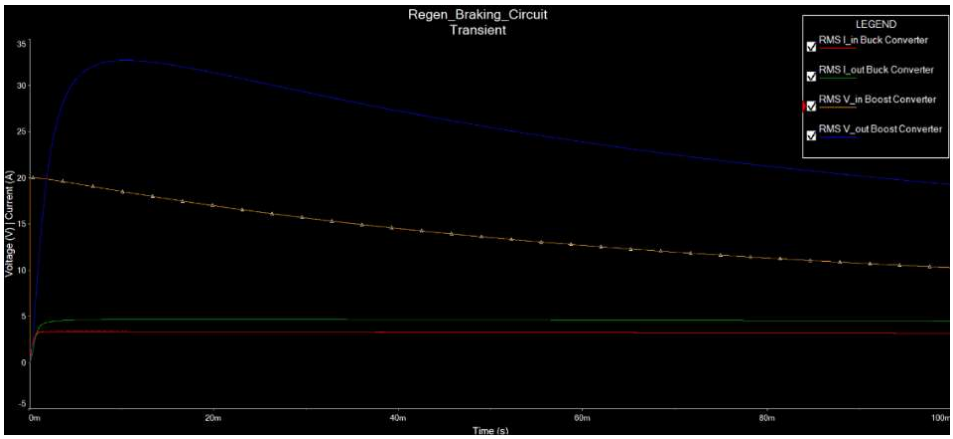

Figure 12. DC-DC Converters effect on voltage and current

Part C: Practical Limitations and Improvements

As practical limitations found during the development of this assignment, the simulations did not consider heat losses, wire impedance or capacitor voltage limits. Transistors also were treated as ideal, ignoring switching delays and conduction losses. Additionally, the control system, in the form of manual switches, was assumed to respond without input delay.

The inverter´s performance is limited by the switching losses present on the transistor diodes. Although the use of both MOSFET and IGBT transistors is possible, the use of N-channel enhancement MOSFET transistors will improve the efficiency of the circuit, due to the lower switching losses (Emadi A., 2015).

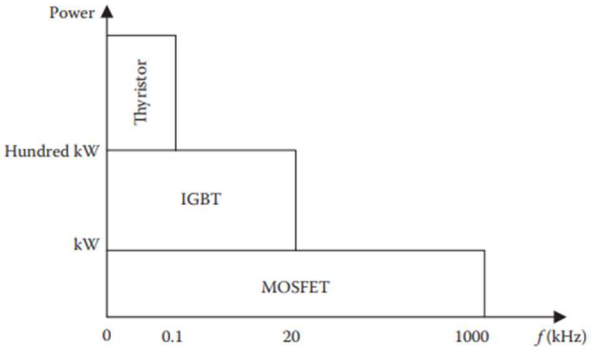

Figure 13. Power rating and switching frequency range of switching devices

It has been found that induced harmonics from the AC components can cause distortion on the output voltage and interference with the controllers (Carbone R., 2002); to solve this, filters can be placed onto the output side of the inverter (Yang C., 2023).

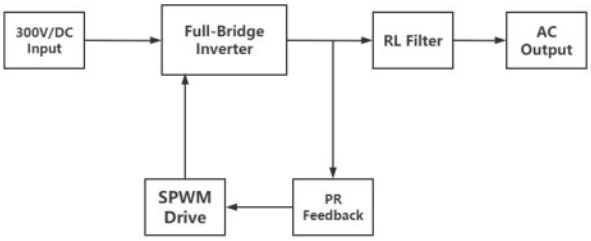

Figure 14. Block diagram of proposed filter structure

To ease the simulation process for the regenerative braking system, the switches were controlled manually, instead of relying on an Electronic Control Unit. To improve the system performance, an electronic controller should be paired to the driver's inputs controller (Nama T., 2022).

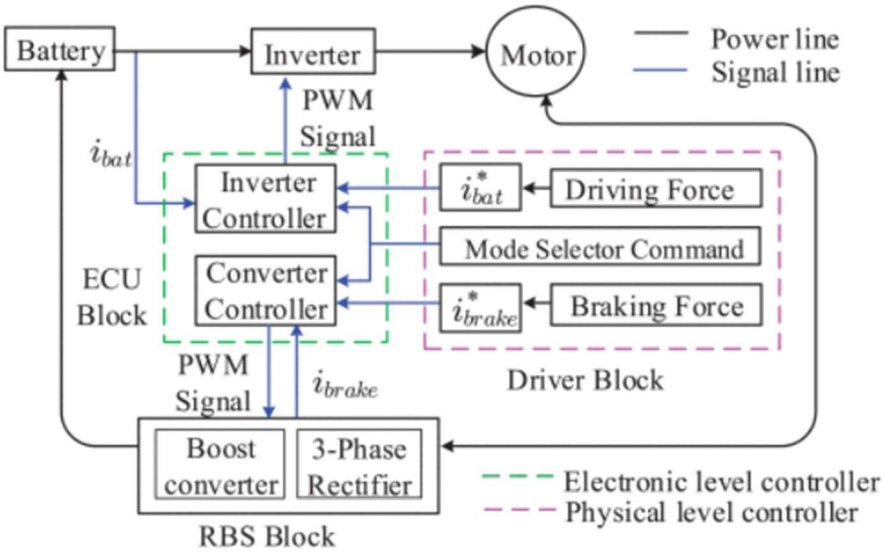

Figure 15. Single line block diagram of the proposed control architecture

In order to improve the regenerative braking system´s performance on an EV vehicle, an interleaved bidirectional Buck/Boost DC-DC converter is proposed, as it allows a more compact design, while improving the system´s efficiency and voltage control, ensuring the stability and reliability of the system (Gangadhar M., 2023).

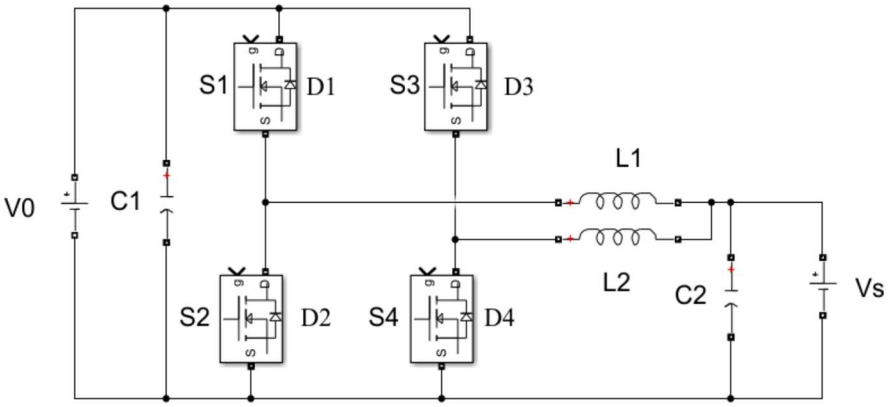

Figure 16. Diagram of the proposed interleaved bidirectional Buck/Boost DC-DC converter

Conclusion

During this assignment, the design, simulation and circuit evaluation of a DC-AC inverter and a regenerative braking system provided a deeper understanding of their operation, performance, limitations and differences between the various types of possible designs. Through circuit modelling, the inverter's switching process, waveform generation, and modulation techniques were analyzed, highlighting the importance of switching strategies, transistor´s power quality control and the application of the maximum power transfer theorem. Through a proof-of-concept design, the regenerative braking system was also examined, allowing a deep understanding of how energy can be recovered, stored and managed, using ultracapacitors and DC-DC converters, in order to improve power flow management between the regenerative braking phase and the power output phase.

The performance evaluation identified key efficiency challenges, such as switching losses, harmonic distortion, and voltage regulation issues. It was found that, for low power systems, N-channel MOSFETs reduce switching losses the most, improving efficiency, while passive and active filters help minimize harmonics and enhance output quality. Additionally, simulations confirmed that battery State-of-Charge and ultra-capacitor behaviour significantly affect the motor´s torque response and system stability, emphasizing the need for optimized control strategies and well thought out capacitance and inductance values.

Through this work, a deep understanding of power electronics, energy storage management, and system optimization was developed, together with an understanding of problems that may arise while designing a circuit and how to solve them. It was learned that precise control over power flow and switching behaviour enhances system efficiency and signal reliability on both DC-DC converters and DC-AC inverter circuits. Future improvements should include the design of a bidirectional regenerative braking system circuit, advanced control algorithms to substitute the manual switches used on the regenerative braking circuit, implementation of filtering techniques, and real hardware implementation to validate the circuits simulation results.

References

Bird, J. (2021) *Electrical Circuit Theory and Technology*. 7th edn. Abingdon: Routledge.

Emadi, A. (2015) *Advanced Electric Drive Vehicles: Energy, Power Electronics, and Machines.* Boca Raton: CRC Press.

Fraile Mora, J. (2012) *Circuitos eléctricos.* Madrid: McGraw-Hill.

García, J. (2023) *Encyclopaedia of Electrical and Electronic Power Engineering.* Amsterdam: Elsevier.

Madhumitha, G., Uppara, R. and Priya, S. (2023) *Comparative Analysis of Bidirectional Buck/Boost DC-DC Converter and Interleaved Bidirectional Buck/Boost DC-DC Converter for EV Applications.* Available at: https://www.riverpublishers.com/pdf/ebook/chapter/RP_P9788770229630C8.pdf

The Engineering Mindset (2020) *Power inverters explained.* Available at: https://theengineeringmindset.com/power-inverters-explained/

ScienceDirect (2022) *Sinusoidal Pulse Width Modulation (SPWM).* Available at: https://www.sciencedirect.com/topics/engineering/sinusoidal-pulse-width-modulation

Gopalan Colleges (n.d.) *Power Electronics – Course Material.* Available at: https://www.gopalancolleges.com/gcem/course-material/ece/course-plan/sem-VII/power-electronics-10EC73.pdf

Tennessee Tech University (n.d.) *Power Electronics - Chapter 4.* Available at: https://www.tntech.edu/engineering/pdf/cesr/ojo/asuri/Chapter4.pdf

Ojo, O. (2004) The generalized discontinuous PWM scheme for three-phase voltage source inverters, *IEEE Transactions on Industrial Electronics*, 51(6), pp. 1280–1289. Available at: https://ieeexplore.ieee.org/document/1360067

Abdallah, M. N., Sarkar K. T. and Salazar M. P. (2016). Maximum power transfer versus efficiency, *IEEE*. Available at: https://ieeexplore.ieee.org/abstract/document/7695800

Hedlund, M. (2010). Design and construction of a bidirectional DCDC converter for an EV application, *Uppsala University*. Available at: https://urn.kb.se/resolve?urn=urn:nbn:se:uu:diva-119916

Mishra, S. and Pattnaik, S. (2023) A battery-ultracapacitor based electric vehicle with regenerative braking system, *2023 5th International Conference on Energy, Power and Environment: Towards Flexible Green Energy Technologies (ICEPE)*. Available at: https://ieeexplore.ieee.org/document/10201541

Nama, T., et al. (2022) Design, modeling and hardware implementation of regenerative braking for electric two-wheelers for hilly roads, *IEEE*. Available at: https://ieeexplore.ieee.org/document/9987244